Article

Hawking Radiation and Lifetime of Primordial Black Holes in Braneworld

Bobur Turimov [1,2,3,4,*], Akhror Mamadjanov [5] and Ozodbek Rahimov [2,3,6]

1   School of Applied Mathematics, New Uzbekistan University, Mustaqillik Avenue 54, Tashkent 100007, Uzbekistan
2   School of Engineering, Akfa University, Milliy Bog Street 264, Tashkent 111221, Uzbekistan; rahimov@astrin.uz
3   Ulugh Beg Astronomical Institute, Astronomy Street 33, Tashkent 100052, Uzbekistan
4   Department of Civil System Engineering, Ajou University in Tashkent, Asalobod Street 113, Tashkent 100204, Uzbekistan
5   Namangan Engineering-Construction Institute, Islom Karimov Street 12, Namangan 160103, Uzbekistan; mamadjanov3084@gmail.com or mamadjanov-ai84@umail.uz
6   Tashkent State Technical University named after Islam Karimov, Tashkent 100095, Uzbekistan
*   Correspondence: bturimov@astrin.uz

Abstract: The paper explores the thermodynamic properties of primordial black holes (PBHs) in the braneworld. Specifically, the researchers examined Hawking radiation and the lifetime of PBHs. Through their analysis, an exact analytical expression for the Bekenstein–Hawking entropy, temperature, and heat capacity was derived. Their findings suggest that the lifetime of PBHs in the early universe is reduced by at least one order of magnitude, ultimately leading to their evaporation. This could explain why we have not observed the final rapid evaporation of PBHs in the recent epoch of the universe.

Keywords: primordial black hole; braneworld; Hawking radiation; lifetime

1. Introduction

Primordial black holes (PBHs) are a hypothetical type of black hole believed to have formed in the initial period of the universe, specifically during the radiation-dominated era that occurred over a second after the Big Bang. There are several potential mechanisms for the formation of PBHs, including inflation [1–8], the collapse of large density fluctuations [9,10], phase transition [11–18], cosmic string loops [19,20], and bubble collisions [21–23]. The possibility of similar black holes was first suggested by Zeldovich [24], and the theory of PBHs was later extended by Hawking [9]. Unlike black holes created from stellar gravitational collapse, PBHs can have masses significantly smaller or larger than the stellar mass. Their mass is approximately equal to the horizon mass, that can be expressed as [25]

$$M \sim \frac{c^3 t}{G} \sim 10^{15} \left(\frac{t}{10^{-23} s} \right) \text{g} \, . \tag{1}$$

According to Hawking, the Planck mass, which is relevant on the Planck time scale of $t_{\text{Pl}} \sim 10^{-43}$ s, would be approximately $M \geq 10^{-5}$ g. In comparison, a supermassive black hole (SMBH) with a mass of $M \sim 10^6 M_\odot$ could form within just one second, or ~ 1 s, after the Big Bang. According to Hawking [26], PBHs radiate thermally and the evaporation timescale is calculated by [27]

$$\tau \sim \frac{\hbar c^4}{4 \pi G^2} M^3 \sim 10^{10} \left(\frac{M}{10^{15} \text{g}} \right)^3 \text{Gyr} \, . \tag{2}$$

However, the lifetime of PBHs with a mass of around 10^{13}g is approximately equal to the age of the present universe. The Hawking temperature is defined as the temperature that a black hole would have to have in order to emit radiation at the same rate that it is losing mass due to Hawking radiation. Alternatively, the temperature of the black hole (Hawking temperature) can be evaluated via the surface gravity method at the horizon:

$$T = \frac{\kappa_g}{2\pi}\,, \qquad \kappa_g = \frac{1}{2}\frac{dg_{tt}}{dr}\bigg|_{r=r_h}\,, \tag{3}$$

where κ_g is the surface gravity factor and r_h is the radius of the event horizon of the black hole.

PBHs are sometimes classified as massive compact halo objects (MACHOs). They have been proposed as a possible explanation for the dark matter (DM) problem, which is one of the most significant and interesting subjects in modern cosmology and astrophysics. However, various astrophysical and cosmological observations have placed tight limits on the abundance of PBHs, making it unlikely that they contribute significantly to DM across most of the possible mass range. Despite this, PBHs are still considered to be potential candidates for the seeds of supermassive black holes with a mass range of $M \sim 10^6$–$10^{10} M_\odot$ at the centers of massive galaxies, as well as intermediate-mass black holes with a mass range of $M \sim 50$–$100 M_\odot$ [28].

Gravitational waves emitted by the merger of a binary system of black holes, as observed by the LIGO/VIRGO collaborations, have led three separate groups of scientists to independently propose a potential primordial origin for the detected black holes [29–31]. Two of these groups have found that the merging rates of the binary system, as inferred by LIGO, align with a scenario where all dark matter (DM) in the universe consists of Primordial Black Holes (PBHs). However, the third group argues that the merging rates are inconsistent with this scenario, suggesting that PBHs may only contribute to less than approximately 1% of the total DM. The unexpectedly large mass of the black holes detected by LIGO has sparked renewed interest in PBHs within the mass range of 1 to 100 times the mass of the Sun ($M_\odot$). However, an ongoing debate persists regarding the exclusion of this mass range based on other observations. These include the absence of stellar microlensing, anisotropies in the cosmic microwave background, the sizes of faint dwarf galaxies, and the lack of correlation between X-ray and radio sources toward the galactic center. Notably, in a recent paper by Kashlinsky [32], the author suggests that the observed spatial correlations in unresolved gamma-ray and X-ray background radiation could potentially be attributed to PBHs with similar masses, assuming their abundance is comparable to that of dark matter (DM). While some propose the evaporation of PBHs as a possible explanation for gamma-ray bursts, this scenario is generally regarded as unlikely. PBHs have also been suggested as a solution to other problems, such as the dark matter problem, the cosmological domain wall problem [33], and the cosmological monopole problem [34]. Since PBHs can have varying sizes and are not necessarily small, they may have played a role in the later formation of galaxies. The impact of accreting matter on PBH evaporation has been investigated in a study by Khlopov [35].

The purpose of this study is to investigate the Hawking radiation and lifespan of PBHs in the context of the braneworld scenario. Braneworld models are a class of theoretical models in physics and cosmology that propose the existence of additional spatial dimensions beyond the three that we experience in our everyday lives. These models suggest that our universe may be a four-dimensional "brane" (short for "membrane") embedded within a higher-dimensional space-time called the "bulk". The idea of braneworlds emerged from the study of string theory, which posits that fundamental particles are not point-like, but instead are tiny one-dimensional "strings" that vibrate at different frequencies. In some versions of string theory, these strings are confined to a four-dimensional brane, while gravity (which is mediated by a hypothetical particle called the graviton) can propagate through the bulk. One of the most well-known braneworld models is the Randall–Sundrum model, proposed by Lisa Randall and Raman Sundrum [36]. This model proposes that our

universe is a brane embedded within a five-dimensional space-time, and that the observed weakness of gravity compared to the other fundamental forces can be explained by the fact that gravity is diluted across the extra dimension. In Ref. [37], the exterior vacuum solutions of the braneworld model for a spherically symmetric and static system were derived. Braneworld models have been the subject of intense research in recent years, as they offer the potential to unify gravity with the other fundamental forces of nature and provide new insights into the nature of dark matter and dark energy. This new class of spherical symmetrical black hole solutions was presented in [38–40].

The braneworld models have been extensively studied in the literature as a potential framework for astrophysical observations. Various tests have been proposed to probe the models at different scales, including gravitational lensing [41–45], motion of test particles around black holes [46–48], optical effects in the space-time of rotating braneworld black holes [49], electromagnetic fields around magnetized neutron stars [50–55], and quasiperiodic oscillations (QPOs) in neutron star binary systems [56,57]. Additionally, the flux energy and thermal spectrum from accretion disks around various classes of static and rotating braneworld black holes have been investigated in Refs. [58,59]. The weak-field deflection angle and bending of light around massive braneworld black holes have also been studied [60,61]. Additionally, the possibility of detecting braneworld black holes through their gravitational wave emissions has also been investigated. In Ref. [62], the quasinormal modes of black holes in the braneworld scenario were studied and compared with those in general relativity.

The paper is arranged as follows. Section 2 delves into the investigation of the lifetime of PBHs in the braneworld. Moving on to Section 3, we present the fundamental equations that describe the thermodynamics of PBHs in the braneworld. In Section 4, we discuss the emission rate and gray-body factor of PBHs in the braneworld. A summary of the results obtained is provided in Section 5. Throughout the paper, we adopt the convention of a metric with a signature of $(-,+,+,+)$, and we use geometrized units where $G = c = \hbar = k = 1$. Greek indices range from 0 to 3, while Latin indices range from 1 to 3.

2. Lifetime of PBH in the Braneworld

In this section, we investigate the lifetime of PBHs in the braneworld and examine the impact of brane tension on the lifespan of static black holes. The space-time metric for a spherically symmetric, static black hole in the braneworld is given as [37].

$$ds^2 = -f(r)dt^2 + \frac{dr^2}{f(r)} + r^2(d\theta^2 + \sin^2\theta d\phi^2) \,, \tag{4}$$

with

$$f(r) = 1 - \frac{2M}{r} + \frac{Q^*}{r^2} \,, \tag{5}$$

where M represents the total mass of the primordial black hole (PBH) and Q^* denotes the brane charge parameter, also known as the "Weyl charge", which is negatively identified ($Q^* < 0$). (For more comprehensive information, refer to [63]). For the sake of convenience in subsequent calculations, we introduce a new positive brane parameter, denoted as $b^2 = -Q^*$. Consequently, the sign of the last term in the metric function $f(r)$ will be altered. The radius of the outer horizon of a black hole can be determined, from the largest solution of $f = 0$, as

$$r_+ = M + \sqrt{M^2 + b^2} \geq 2M \,, \tag{6}$$

which is greater then Schwarzschild radius. The dependence of the event horizon from the brane parameter is illustrated in Figure 1. The dimensional event horizon is presented in the left panel and dimensionless one is given in the right panel of the Figure 1.
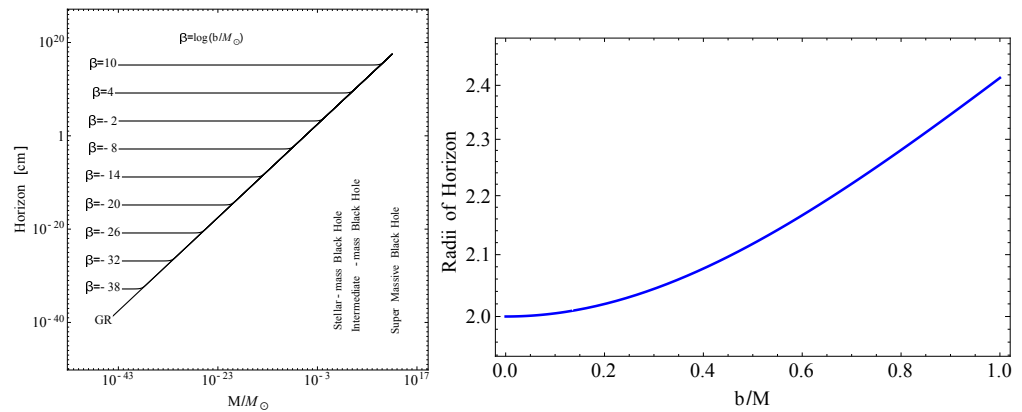
Figure 1. (**Left panel**) Dependence of radius of horizon of PBH form its mass for the different values of brane tension. (**Right panel**) Dependence of radius of horizon of PBH form brane tension parameter b/M.

Recalling Equation (3), the Hawking temperature over the surface of the black hole in the braneworld can be obtained as

$$T = \frac{\sqrt{M^2 + b^2}}{2\pi \left(M + \sqrt{M^2 + b^2} \right)^2} \leq \frac{1}{8\pi M} \; . \tag{7}$$

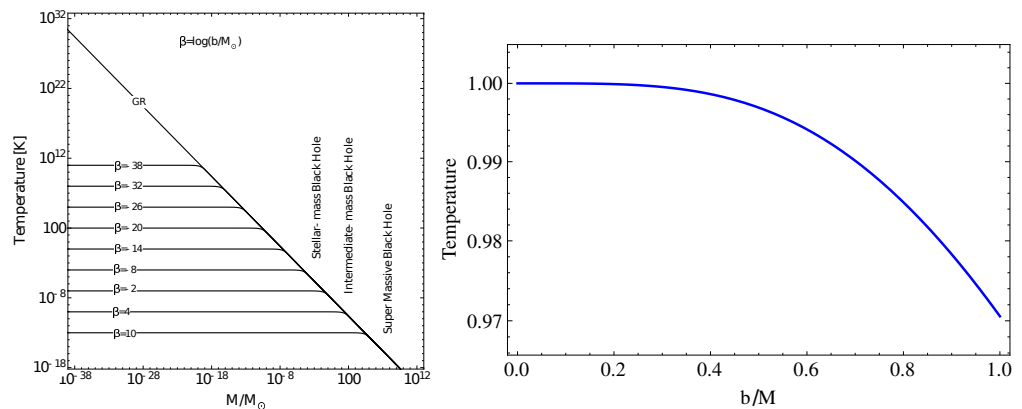Figure 2 draws the dependence of the Hawking temperature from the brane parameter.

Figure 2. (**Left panel**) Dependence of temperature of PBH from its mass for the different values of brane parameter. (**Right panel**) Dependence of temperature of PBH from brane parameter b/M.

The most important parameter of a PBH is its lifetime. The lifetime of a primordial black hole (PBH) depends on its initial mass and the mechanisms by which it can lose mass. PBHs are hypothetical black holes that are thought to have formed in the early universe shortly after the Big Bang. The rate of energy loss from a PBH in the braneworld can be approximated with the Stephan–Boltzmann radiation law as

$$\frac{dM}{dt} \simeq \sigma A T^4 = 4\pi \sigma r_+^2 T^4 \; , \tag{8}$$

where $\sigma = \pi^2/60$ is the Stefan-Boltzmann constant, and A represents the surface area of the black hole horizon. By utilizing the expressions for the temperature (7) and the radius of the horizon (6), Equation (8) can be rewritten in the following form:

$$\frac{dM}{dt} = -\frac{1}{240\pi} \frac{\left(M^2 + b^2 \right)^2}{\left(M + \sqrt{M^2 + b^2} \right)^6} \; . \tag{9}$$

Now one can easily calculate the lifetime of a PBH in terms of brane charge parameter:

$$\tau = -240\pi \int_M^0 \frac{dM}{(M^2 + b^2)^2} \left(M + \sqrt{M^2 + b^2} \right)^6 . \tag{10}$$

Before evaluating the integral (10), the brane parameter b can be considered a constant, denoted as $b = $ const, independent of the mass of the PBH. Evaluating the integral (10) from M to 0 yields the lifetime τ of the PBH. In the case where $b = $ const, one can obtain the following expression:

$$\tau = 2560\pi M^3 \left[1 - \frac{3b^2}{2M^2} - \frac{3b^4}{64M^2(b^2 + M^2)} \right.$$
$$\left. + \frac{16M^4 - 41b^4 - 16b^2M^2}{16M^3\sqrt{b^2 + M^2}} + \frac{105b^3}{64M^3} \tan^{-1}\left(\frac{M}{b} \right) \right] . \tag{11}$$

Note that, in this case, the general relativistic limit of the lifetime takes the standard value as obtained in Ref. [64]:

$$\tau_0 = \lim_{b \to 0} \tau = 5120\pi M^3 . \tag{12}$$

The small brane charge parameter ratio of the lifetime of the PBH takes the form

$$\tau = \tau_0 \left(1 - \frac{3b^2}{2M^2} + \frac{105\pi b^3}{256M^3} \right) + \mathcal{O}\left(b^4 \right) , \tag{13}$$

which shows that the lifetime of the PBH will be shorter in the braneworld scenario.

Figure 3 illustrates the fractional lifetime for different values of the brane charge parameter compared to that of a Schwarzschild black hole (i.e., $b = 0$). The dependence on b clearly has an impact on the lifetime of these black holes. It is evident that when $b = $ const, a value of $b = 0.5M$ reduces the PBH's lifetime by approximately 30%.

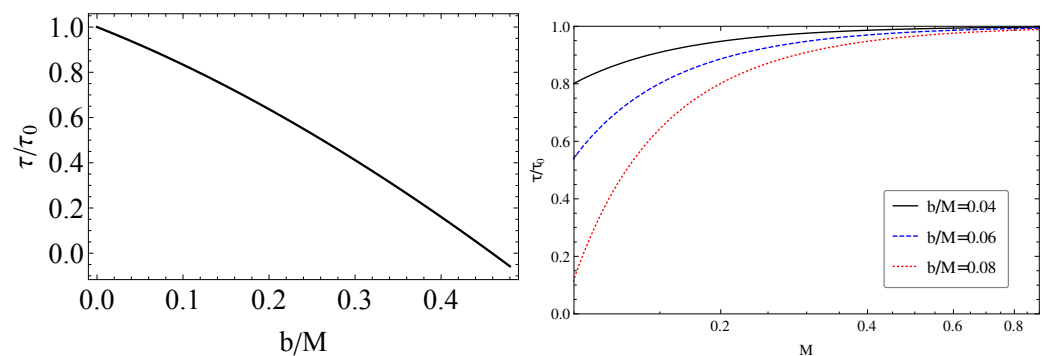**Figure 3.** (**Left panel**) Fractional lifetime of PBH is a function of brane charge parameter b/M. (**Right panel**) Fractional lifetime of PBH is a function of its mass for different values of brane charge parameter.

3. Thermodynamic Properties of PBH in the Braneworld

In this section we briefly study thermodynamic properties of the black hole in the braneworld. The entropy of a black hole is a measure of the amount of disorder or randomness associated with its microscopic degrees of freedom. According to the laws of thermodynamics, any physical system that has a temperature must have an associated entropy, which measures the degree of disorder in the system. In the case of black holes, the concept of entropy was first introduced by Stephen Hawking, who showed that black holes have a nonzero entropy despite being completely black and featureless objects. According to Hawking's calculations, the entropy of a black hole is proportional to its surface

area, rather than its volume or mass, as one might expect. The surface of an outer horizon can be found as $A = 4\pi r_+^2$. Unlike the temperature, the entropy of the black hole can be modified when the action is expanded in a power of Riemann tensor. One of the simplest examples is Gauss–Bonnet action [65]. There will be an additional term of entropy of a black hole when a cosmological term is in action. This arises due to the outer horizon r_+ and cosmological horizon r_c, which can be found in [66]. However, in the braneworld, there is no cosmological term or higher order Riemann tensor. Therefore, one can immediately use the simple expression $S = A/4$ for entropy of the brany black hole. Once we have the surface of the horizon then the area entropy of the black hole can be easily calculated as

$$S = \frac{A}{4} = \pi \left(M + \sqrt{M^2 + b^2} \right)^2 \geq 4\pi M^2 \,. \tag{14}$$

As we shown that the horizon of black hole increases in the presence of the brane. Therefore, the area of horizon also increases that means the entropy of black hole should increases. Figure 4 shows dependence of the entropy from the brane parameter.
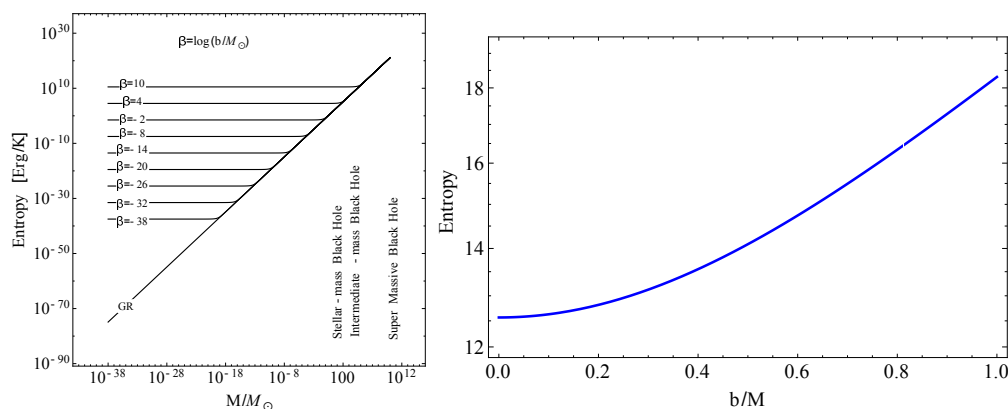

Figure 4. (**Left panel**) Dependence of entropy of PBH (in Equation (14)) from its mass for the different values of brane tension. (**Right panel**) Dependence of entropy of PBH from brane tension parameter b/M.

The free energy of a black hole is a thermodynamic quantity that characterizes the ability of the black hole to do work, and is defined as the difference between its total energy and its entropy multiplied by its temperature: $F = E - TS$, where F is the free energy, E is the total energy, T is the temperature, and S is the entropy. In the case of black holes, the free energy is closely related to the thermodynamic stability of the black hole. A black hole is said to be thermodynamically stable if its free energy is negative, indicating that it can release energy and move towards a lower energy state. Conversely, if the free energy is positive, the black hole is said to be thermodynamically unstable, and it can absorb energy and grow in size. The free energy of a black hole can be computed using the Bekenstein–Hawking formula for the entropy and the formula for the temperature of a black hole. Using Equation (7), one can obtain an expression for the free energy of a black hole in terms of its mass and the fundamental constants of nature. According to the definition of free energy $F = M - TS$ of the thermodynamic system, one can have

$$F = M - TS = M - \frac{1}{2}\sqrt{M^2 + b^2} \,, \tag{15}$$

As one can see from Equation (15) the free energy F of the thermodynamic system can be negative, i.e., $F < 0$ for the values of brane charge parameter $b \geq \sqrt{3}M$. On the other hand, the absence of brane charge parameter one can obtain $F = M/2$, that is free energy in Schwarzschild space-time. Figure 5 shows dependence of the free energy from the brane tension. As we mentioned before, it decreases due the brane effect.
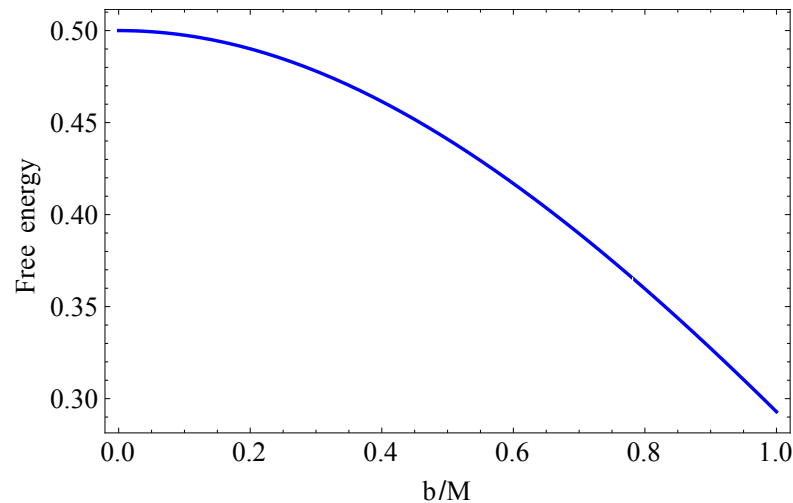
Figure 5. Dependence of free energy from brane tension b/M.

Now one can see that in an isoelastic process, the specific heat can be found as

$$C_V = T\frac{\partial S}{\partial T} = T\frac{\partial S}{\partial M}\left(\frac{\partial T}{\partial M}\right)^{-1}$$

$$= -\frac{2\pi\sqrt{M^2 + b^2}\left(M + \sqrt{M^2 + b^2}\right)^2}{\left(2\sqrt{M^2 + b^2} - M\right)}. \tag{16}$$

We now differentiate both sides of Equation (14) and obtain the following simple formula

$$dS = \frac{2\pi\left(M + \sqrt{M^2 + b^2}\right)^2}{\sqrt{M^2 + b^2}}dM = \frac{dM}{T}, \tag{17}$$

which allows us to write $dQ = dM = TdS$, (indeed it is correct if we restore the speed of light $dQ = c^2 dM$), where dQ is the heat energy, and it is always lost due to evaporation of the PBH $\Delta Q = \Delta M = M - M' > 0$, where M and M' are the masses of the initial and final stage of PBH.

On the other hand, the heat lost during a temperature change dT can also be expressed as $dQ = \mathcal{C}MdT$, which allows us to find the specific heat capacity of the PBH:

$$\mathcal{C} = \frac{dQ}{MdT} = \frac{dM}{MdT}, \tag{18}$$

and

$$\mathcal{C} = -\frac{2\pi\sqrt{M^2 + b^2}\left(M + \sqrt{M^2 + b^2}\right)^2}{M\left(2\sqrt{M^2 + b^2} - M\right)}, \tag{19}$$

From Equations (16) and (19), one can easily see that the specific heat and the heat capacity can be related as $C_V = \mathcal{C}M$. Figure 6 draws the dependence of the specific head of the black hole from the brane parameter. It is shown that the specific heat of black hole increases due to the brane parameter.
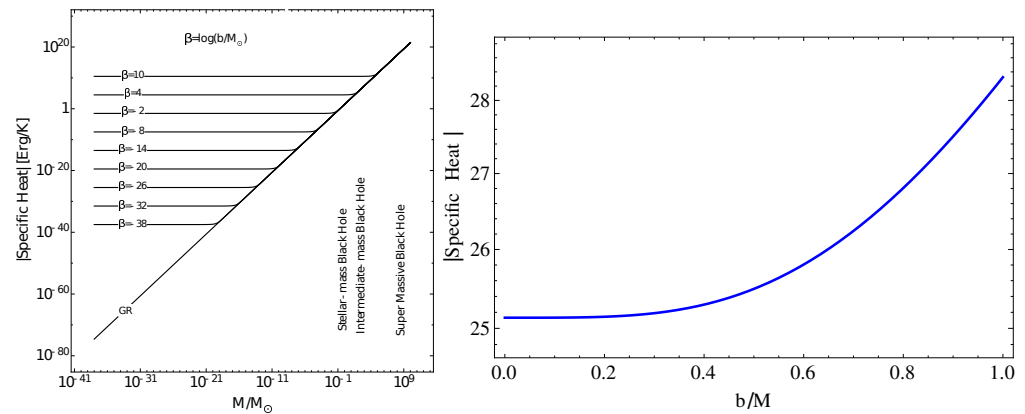
Figure 6. (**Left panel**) Dependence of specific heat of PBH from its mass for the different values of brane tension. (**Right panel**) Dependence of specific heat of PBH from brane tension parameter b/M.

4. Emission Rate and Grey-Body Factor

This section is devoted to the calculation of the emission rate of PBHs and grey-body factor. The grey-body factor characterizes the efficiency of a black hole to emit Hawking radiation. It is a dimensionless quantity that ranges from 0 to 1, with 1 being a perfectly efficient emitter and 0 being a completely absorbing body that does not emit any radiation at all. The grey-body factor takes into account the fact that not all the radiation generated by the black hole will be able to escape due to the gravitational attraction of the black hole itself. The reflection coefficient is the ratio of the reflected wave amplitude to the incident wave amplitude and depends on the frequency of the radiation, the black hole mass, and the spin of the emitted particles. It is well accepted that black holes are thermal systems: they have an associated temperature and entropy and therefore radiate. The differential emission rate of Hawking radiation in the energy range $(\omega, \omega + \delta\omega)$ is [67–70]

$$\frac{dE}{dt} = \sum_{\ell} \sigma_{\ell}(\omega) \frac{d\mathbf{k}dA}{\exp\left(\omega/T\right) - (-1)^{2s}} , \tag{20}$$

where dA is the infinitesimal surface area, T is the temperature of PBH, s is the spin weight, $\mathbf{k}$ is the momentum of the emitted particle and $\sigma_{l}(\omega)$ is the absorption cross section which is often called grey-body factor. Our aim is to calculate the grey-body factor for emitted particle from PBHs through the Hawking radiation. Obviously, it is difficult to obtain an analytical expression for the grey-body factor; however one can use semi-analytical approach suggested in Refs. [71–75].

In terms of the tortoise coordinate x, the Regge–Wheeler equation can be written as [71,74,76]

$$\frac{d^2\Psi}{dx^2} = \left[\omega^2 - V(r)\right]\Psi , \tag{21}$$

where ω is the frequency particle. The tortoise coordinate can be found from the following expression

$$\frac{dr}{dx} = f(r) = 1 - \frac{2M}{r} - \frac{b^2}{r^2} , \tag{22}$$

the effective potential, $V(r)$, in (21), has the form

$$V(r) = f(r)\left[\frac{\ell(\ell+1)}{r^2} + \frac{f'(r)}{r}(1 - s^2)\right] , \tag{23}$$

where ℓ is the specific angular momentum. Keep in mind that, in the case of the tensor field (gravitational perturbation, i.e., $s = 2$), Equation (23) will be different, since the metric (4) in not vacuum solution, there are should be contribution from non-zero components of the

energy-momentum tensor, that is why in the paper we consider Regge–Wheeler equation for the scalar ($s = 0$) and vector ($s = 1$) fields.

The radial dependence of the effective potential for two cases of scalar ($s = 0$) and vector ($s = 1$) fields for the different values of brane tension parameter is drawn in Figure 7. From Figure 7 one can easily see that the maxima of the effective potential for the scalar field (solid lines) is larger with compare to that for the vector field (dashed lines).
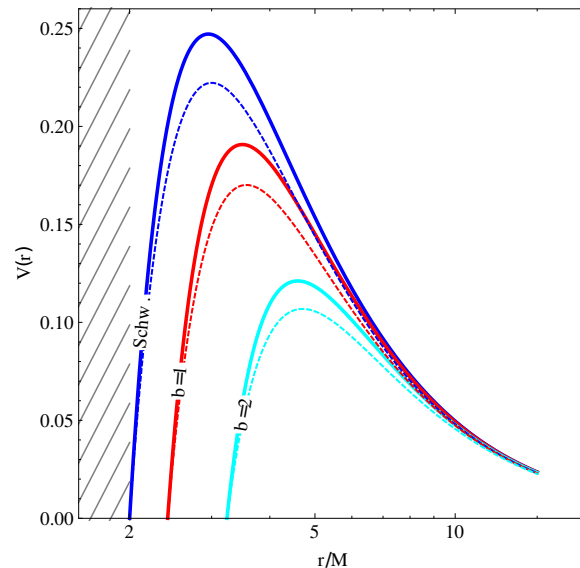

Figure 7. (Color online) Radial dependence of the effective potential for the different values of brane tension parameter b/M at $\ell = 2$. Solid lines represent scalar field ($s = 0$) while dashed lines vector field ($s = 1$) one.

The grey-body factor or transmission probability can be expressed as [71]

$$\mathcal{T} \geq \cosh^{-2}\left\{ \int_{-\infty}^{\infty} \vartheta(x)dx \right\}, \tag{24}$$

on the other hand, the reflection coefficient, $\mathcal{R}$, can be found from the relation, $\mathcal{T} + \mathcal{R} = 1$. More precisely, it can be written as

$$\mathcal{R} \leq \tanh^{2}\left\{ \int_{-\infty}^{\infty} \vartheta(x)dx \right\}, \tag{25}$$

where "cosh" and "tanh" are, respectively, hyperbolic cosine and hyperbolic tangent functions. The function ϑ can be found as [71]

$$\vartheta(x) = \frac{\sqrt{h'^2(x) + [\omega^2 - V(x) - h(x)]^2}}{2h(x)}, \tag{26}$$

where $h(x)$ is the some positive function, $h(x) > 0$, which satisfies the following conditions; otherwise it can be arbitrary. It is difficult to find the analytical form of the grey-body factor, but one can find semi-analytical expression in some approximation. In order to find the semi-analytical expression, one can study two different scenarios:

First case: We first consider the following case, $h = \omega$, the grey-body factor can be expressed as

$$\mathcal{T} \geq \cosh^{-2}\left\{ \frac{1}{2\omega} \int_{-\infty}^{\infty} V(x)dx \right\} \tag{27}$$

$$= \cosh^{-2}\left\{ \frac{1}{2\omega} \int_{r_+}^{\infty} \left[\frac{\ell(\ell+1)}{r^2} + \frac{f'(r)}{r}\left(1 - s^2\right) \right]dr \right\},$$

now integral in (27) is trivial, it can be easily integrated. The transmission coefficient takes the form

$$\mathcal{T} = \cosh^{-2}\left(\frac{\eta M r_+ + \xi b}{2\omega r_+^3}\right),$$ (28)

where $\eta = (\ell+1)^2 + \ell^2 - s^2$ and $\xi = \ell(\ell+1) + 2(1-s^2)/3$.

The dependence of the transmission and reflection coefficients from the frequency for the different values of the brane tension parameter is plotted in Figure 8 (left panel). It is shown that the curve of transmission and reflection coefficients intersect each other in the braneworld scenario even in the low frequency regime. In the right panel in Figure 8, the dependence of the transmission and reflection coefficients from the brane tension parameters for the different fields corresponding to $s = 0$ and $s = 1$ is illustrated. It is shown that in the case of scalar field ($s = 0$), the transmission and reflection coefficients lines can be intersected at the larger values of brane tension parameter in comparison with the vector field case.
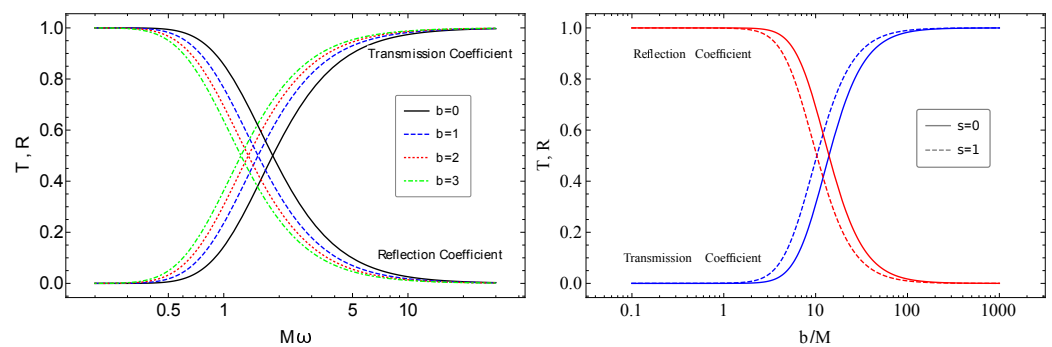

Figure 8. (**Left panel**) The transmission and reflection coefficients of PBH for the different values of brane tension at $\ell = 2$. (**Right panel**) Dependence of transmission and reflection coefficients of PBH from the brane tension for the scalar and vector fields at $\ell = 1$.

Second case: It can be assumed that the function $h(x)$ takes the form $h = \sqrt{\omega^2 - V}$ and obtain

$$\mathcal{T} \geq \cosh^{-2}\left\{\frac{1}{2}\int_{-\infty}^{\infty}\frac{h'(x)}{h(x)}dx\right\}$$
$$= \cosh^{-2}\left\{\ln\frac{h_0}{h_\infty}\right\}$$
$$= \cosh^{-2}\left\{\ln\frac{\sqrt{\omega^2 - V_0}}{\omega}\right\},$$ (29)

here, V_0 is the maximum value of the effective potential at point $r_0 = \frac{1}{2}\left(\sqrt{8b^2 + 9M^2} + 3M\right)$ for spin zero ($s = 0$) field, but for spin zero field extremum point for the effective potential will be complicated. That is why we will not include here. Finally, the transmission and reflection coefficients take the form

$$\mathcal{T} \geq 1 - \frac{V_0^2}{(2\omega^2 - V_0)^2}, \qquad \mathcal{R} \leq \frac{V_0^2}{(2\omega^2 - V_0)^2}.$$ (30)

Note that previous calculations can be easily done for the tensor ($s = 2$) fields. However, in that case, one has to make careful calculations, including the source term. This is because the black hole solution in the presence of the brane is not a vacuum solution.

5. Conclusions

The primary objective of this paper was to delve into the thermodynamic properties of PBHs, specifically focusing on their Hawking radiation and evaporation within the braneworld model. The key outcomes of this study are as follows:

- We have studied the thermodynamic properties of PBHs within the braneworld model, taking into account the effect of brane tension. Through our analysis, we were able to derive exact analytical expressions for various thermodynamic quantities including temperature, entropy, Bekenstein–Hawking entropy, specific heat, heat capacity, and free energy.
- We have also investigated the impact of the braneworld scenario on the Hawking radiation and the lifetime of PBHs. Our findings indicate that PBHs in the early universe experienced a shortened lifetime by at least one order of magnitude, leading to early evaporation. This early evaporation could explain the absence of specific high-energy bursts associated with PBH evaporation in the recent epoch of the universe.
- Finally, we have investigated the grey-body factor, which characterizes the efficiency of a black hole to emit Hawking radiation, by determining the transmission and reflection coefficients. To obtain these coefficients, we have employed the Regge–Wheeler equation for massless scalar ($s = 0$) and vector ($s = 1$) fields. Our analysis has revealed that in the braneworld scenario, the transmission and reflection coefficient curves intersect each other, even in the low frequency regime, which has implications for the behavior of Hawking radiation from PBHs. Moreover, we have found that for the scalar field case, the intersection of the transmission and reflection coefficient curves occurs at larger values of the brane tension parameter compared to the vector field case.

Author Contributions: Conceptualization, B.T.; Methodology, A.M. and O.R.; Software, B.T.; Formal analysis, O.R.; Investigation, B.T. and A.M.; Writing—original draft, B.T.; Writing—review editing, O.R. All authors have read and agreed to the published version of the manuscript.

Institutional Review Board Statement: Not applicable.

Informed Consent Statement: Not applicable.

Data Availability Statement: No associated data is available in the project.

Conflicts of Interest: The authors declare no conflict of interest.

References

1. Ivanov, P.; Naselsky, P.; Novikov, I. Inflation and primordial black holes as dark matter. *Phys. Rev. D* **1994**, *50*, 7173–7178. [CrossRef]
2. Carr, B.J.; Gilbert, J.H.; Lidsey, J.E. Black hole relics and inflation: Limits on blue perturbation spectra. *Phys. Rev. D* **1994**, *50*, 4853–4867. [CrossRef]
3. García-Bellido, J.; Linde, A.; Wands, D. Density perturbations and black hole formation in hybrid inflation. *Phs. Rev. D* **1996**, *54*, 6040–6058. [CrossRef] [PubMed]
4. Yokoyama, J. Formation of MACHO-primordial black holes in inflationary cosmology. *Astron. Astrophys.* **1997**, *318*, 673–679.
5. Yokoyama, J. Chaotic new inflation and formation of primordial black holes. *Phys. Rev. D* **1998**, *58*, 083510. [CrossRef]
6. Yokoyama, J. Formation of primordial black holes in the inflationary universe. *Phys. Rep.* **1998**, *307*, 133–139. [CrossRef]
7. Kawasaki, M.; Yanagida, T. Primordial black hole formation in supergravity. *Phys. Rev. D* **1999**, *59*, 043512. [CrossRef]
8. Alabidi, L.; Kohri, K. Generating primordial black holes via hilltop-type inflation models. *Phys. Rev. D* **2009**, *80*, 063511. [CrossRef]
9. Hawking, S. Gravitationally collapsed objects of very low mass. *Mon. Not. R. Astron. Soc.* **1971**, *152*, 75. [CrossRef]
10. Carr, B.J. The primordial black hole mass spectrum. *Astrophys. J.* **1975**, *201*, 1–19. [CrossRef]

11.   Khlopov, M.Y.; Polnarev, A.G. Primordial black holes as a cosmological test of grand unification. *Phys. Lett. B* **1980**, *97*, 383–387. [CrossRef]

12.   Niemeyer, J.C.; Jedamzik, K. Near-Critical Gravitational Collapse and the Initial Mass Function of Primordial Black Holes. *Phys. Rev. Lett.* **1998**, *80*, 5481–5484. [CrossRef]

13.   Niemeyer, J.C.; Jedamzik, K. Dynamics of primordial black hole formation. *Phys. Rev. D* **1999**, *59*, 124013. [CrossRef]

14.   Jedamzik, K.; Niemeyer, J.C. Primordial black hole formation during first-order phase transitions. *Phys. Rev. D* **1999**, *59*, 124014. [CrossRef]

15.   Nozari, K. A possible mechanism for production of primordial black holes in early universe. *Astropart. Phys.* **2007**, *27*, 169–173. [CrossRef]

16.   Musco, I.; Miller, J.C.; Rezzola, L. Computations of primordial black-hole formation. *Class. Quantum Gravity* **2005**, *22*, 1405–1424. [CrossRef]

17.   Musco, I.; Miller, J.C.; Polnarev, A.G. Primordial black hole formation in the radiative era: Investigation of the critical nature of the collapse. *Class. Quantum Gravity* **2009**, *26*, 235001. [CrossRef]

18.   Musco, I.; Miller, J.C. Primordial black hole formation in the early universe: Critical behaviour and self-similarity. *Class. Quantum Gravity* **2013**, *30*, 145009. [CrossRef]

19.   Hawking, S.W. Black holes from cosmic strings. *Phys. Lett. B* **1989**, *231*, 237–239. [CrossRef]

20.   Polnarev, A.; Zembowicz, R. Formation of primordial black holes by cosmic strings. *Phys. Rev. D* **1991**, *43*, 1106–1109. [CrossRef]

21.   Hawking, S.W.; Moss, I.G.; Stewart, J.M. Bubble collisions in the very early universe. *Phys. Rev. D* **1982**, *26*, 2681–2693. [CrossRef]

22.   Crawford, M.; Schramm, D.N. Spontaneous generation of density perturbations in the early Universe. *Nature* **1982**, *298*, 538–540. [CrossRef]

23.   Kodama, H.; Sasaki, M.; Sato, K. Abundance of Primordial Holes Produced by Cosmological First-Order Phase Transition. *Prog. Theor. Phys.* **1982**, *68*, 1979–1998. [CrossRef]

24.   Zel'dovich, Y.B.; Novikov, I.D. The Hypothesis of Cores Retarded during Expansion and the Hot Cosmological Model. *Astron. Zhurnal* **1966**, *43*, 758.

25.   Carr, B.J.; MacGibbon, J.H. Cosmic rays from primordial black holes and constraints on the early universe. *Phys. Rep.* **1998**, *307*, 141–154. [CrossRef]

26.   Hawking, S.W. Black hole explosions? *Nature* **1974**, *248*, 30–31. [CrossRef]

27.   Carr, B.J.; Kohri, K.; Sendouda, Y.; Yokoyama, J. New cosmological constraints on primordial black holes. *Phys. Rev. D* **2010**, *81*, 104019. [CrossRef]

28.   Clesse, S.; García-Bellido, J. Massive primordial black holes from hybrid inflation as dark matter and the seeds of galaxies. *Phys. Rev. D* **2015**, *92*, 023524. [CrossRef]

29.   Bird, S.; Cholis, I.; Muñoz, J.B.; Ali-Haïmoud, Y.; Kamionkowski, M.; Kovetz, E.D.; Raccanelli, A.; Riess, A.G. Did LIGO Detect Dark Matter? *Phys. Rev. Lett.* **2016**, *116*, 201301. [CrossRef] [PubMed]

30.   Clesse, S.; García-Bellido, J. The clustering of massive Primordial Black Holes as Dark Matter: Measuring their mass distribution with advanced LIGO. *Phys. Dark Universe* **2017**, *15*, 142–147. [CrossRef]

31.   Sasaki, M.; Suyama, T.; Tanaka, T.; Yokoyama, S. Primordial Black Hole Scenario for the Gravitational-Wave Event GW150914. *Phys. Rev. Lett.* **2016**, *117*, 061101. [CrossRef]

32.   Kashlinsky, A. LIGO Gravitational Wave Detection, Primordial Black Holes, and the Near-IR Cosmic Infrared Background Anisotropies. *Astrophys. J. Lett.* **2016**, *823*, L25. [CrossRef]

33.   Stojkovic, D.; Freese, K.; Starkman, G.D. Holes in the walls: Primordial black holes as a solution to the cosmological domain wall problem. *Phys. Rev. D* **2005**, *72*, 045012. [CrossRef]

34.   Stojkovic, D.; Freese, K. A black hole solution to the cosmological monopole problem. *Phys. Lett. B* **2005**, *606*, 251–257. [CrossRef]

35.   Khlopov, M.; Paik, B.; Ray, S. Revisiting Primordial Black Hole Evolution. *Axioms* **2020**, *9*, 71. [CrossRef]

36.   Randall, L.; Sundrum, R. Large Mass Hierarchy from a Small Extra Dimension. *Phys. Rev. Lett.* **1999**, *83*, 3370–3373. [CrossRef]

37.   Dadhich, N.; Maartens, R.; Papadopoulos, P.; Rezania, V. Black holes on the brane. *Phys. Lett. B* **2000**, *487*, 1–6. [CrossRef]

38.   Casadio, R.; Fabbri, A.; Mazzacurati, L. New black holes in the brane world? *Phys. Rev. D* **2002**, *65*, 084040. [CrossRef]

39.   Casadio, R.; Mazzacurati, L. Bulk Shape of Brane-World Black Holes. *Mod. Phys. Lett. A* **2003**, *18*, 651–660. [CrossRef]

40.   Bronnikov, K.; Melnikov, V.; Dehnen, H. General class of brane-world black holes. *Phys. Rev. D* **2003**, *68*, 024025. [CrossRef]

41.   Bozza, V. Gravitational lensing in the strong field limit. *Phys. Rev. D* **2002**, *66*, 103001. [CrossRef]

42.   Eiroa, E.F. Braneworld Black Holes as Gravitational Lenses. *Braz. J. Phys.* **2005**, *35*, 1113–1116. [CrossRef]

43.   Whisker, R. Strong gravitational lensing by braneworld black holes. *Phys. Rev. D* **2005**, *71*, 064004. [CrossRef]

44.   Keeton, C.R.; Petters, A.O. Formalism for testing theories of gravity using lensing by compact objects. III. Braneworld gravity. *Phys. Rev. D* **2006**, *73*, 104032. [CrossRef]

45.   Schee, J.; Stuchlík, Z. Optical Phenomena in the Field of Braneworld Kerr Black Holes. *Int. J. Mod. Phys. D* **2009**, *18*, 983–1024. [CrossRef]

46.   Aliev, A.N.; Gümrükçüoğlu, A.E. Charged rotating black holes on a 3-brane. *Phys. Rev. D* **2005**, *71*, 104027. [CrossRef]

47.   Abdujabbarov, A.; Ahmedov, B. Test particle motion around a black hole in a braneworld. *Phys. Rev. D* **2010**, *81*, 044022. [CrossRef]

48.   Turimov, B. Electromagnetic fields in vicinity of tidal charged static black hole. *Int. J. Mod. Phys. D* **2018**, *27*, 1850092. [CrossRef]

49.　Stuchlík, Z.; Blaschke, M.; Schee, J. Particle collisions and optical effects in the mining Kerr-Newman spacetimes. *Phys. Rev. D* **2017**, *96*, 104050. [CrossRef]

50.　Ahmedov, B.J.; Fattoyev, F.J. Magnetic fields of spherical compact stars in a braneworld. *Phys. Rev. D* **2008**, *78*, 047501. [CrossRef]

51.　Morozova, V.S.; Ahmedov, B.J. Electromagnetic fields of slowly rotating compact magnetized stars in braneworld. *Astrophys. Space Sci.* **2011**, *333*, 133–142. [CrossRef]

52.　Turimov, B.V.; Ahmedov, B.J.; Hakimov, A.A. Stationary electromagnetic fields of slowly rotating relativistic magnetized star in the braneworld. *Phys. Rev. D* **2017**, *96*, 104001. [CrossRef]

53.　Turimov, B.; Ahmedov, B.; Abdujabbarov, A.; Bambi, C. Electromagnetic fields of slowly rotating magnetized compact stars in conformal gravity. *Phys. Rev. D* **2018**, *97*, 124005. [CrossRef]

54.　Rayimbaev, J.; Turimov, B.; Ahmedov, B. Braneworld effects in plasma magnetosphere of a slowly rotating magnetized neutron star. *Int. J. Mod. Phys. D* **2019**, *28*, 1950128. [CrossRef]

55.　Rayimbaev, J.; Turimov, B.; Palvanov, S. Plasma magnetosphere of slowly rotating magnetized neutron star in branewold. *Int. J. Mod. Phys. Conf. Ser.* **2019**, *49*, 1960019. [CrossRef]

56.　Kotrlová, A.; Stuchlík, Z.; Török, G. Quasiperiodic oscillations in a strong gravitational field around neutron stars testing braneworld models. *Class. Quantum Gravity* **2008**, *25*, 225016. [CrossRef]

57.　Stuchlík, Z.; Kotrlová, A. Orbital resonances in discs around braneworld Kerr black holes. *Gen. Relativ. Gravit.* **2009**, *41*, 1305–1343. [CrossRef]

58.　Pun, C.S.J.; Kovács, Z.; Harko, T. Thin accretion disks onto brane world black holes. *Phys. Rev. D* **2008**, *78*, 084015. [CrossRef]

59.　Schee, J.; Stuchlík, Z. Profiles of emission lines generated by rings orbiting braneworld Kerr black holes. *Gen. Relativ. Gravit.* **2009**, *41*, 1795–1818. [CrossRef]

60.　Gergely, L.Á.; Darázs, B. Weak gravitational lensing in brane-worlds. *Publ. Astron. Dep. Eotvos Lorand Univ.* **2006**, *17*, 213.

61.　Gergely, L.Á.; Keresztes, Z.; Dwornik, M. Second-order light deflection by tidal charged black holes on the brane. *Class. Quantum Gravity* **2009**, *26*, 145002. [CrossRef]

62.　Toshmatov, B.; Stuchlík, Z.; Schee, J.; Ahmedov, B. Quasinormal frequencies of black hole in the braneworld. *Phys. Rev. D* **2016**, *93*, 124017. [CrossRef]

63.　Germani, C.; Maartens, R. Stars in the braneworld. *Phys. Rev. D* **2001**, *64*, 124010. [CrossRef]

64.　Hawking, S.W. The quantum mechanics of black holes. *Sci. Am.* **1977**, *236*, 34–40. [CrossRef]

65.　Barvinsky, A.O.; Vilkovisky, G.A. The generalized Schwinger-DeWitt technique and the unique effective action in quantum gravity. *Phys. Lett. B* **1983**, *131*, 313–318. [CrossRef]

66.　Ma, Y.; Zhang, Y.; Zhang, L.; Wu, L.; Huang, Y.; Pan, Y. Thermodynamic properties of higher-dimensional dS black holes in dRGT massive gravity. *Eur. Phys. J. C* **2020**, *80*, 213. [CrossRef]

67.　Hawking, S.W. Black holes and thermodynamics. *Phys. Rev. D* **1976**, *13*, 191–197. [CrossRef]

68.　Hawking, S.W. Particle creation by black holes. *Commun. Math. Phys.* **1976**, *46*, 206. [CrossRef]

69.　Halzen, F.; Zas, E.; MacGibbon, J.H.; Weekes, T.C. Gamma rays and energetic particles from primordial black holes. *Nature* **1991**, *353*, 807–815. [CrossRef]

70.　Chakrabarty, H.; Abdujabbarov, A.; Bambi, C. Scalar perturbations and quasi-normal modes of a nonlinear magnetic-charged black hole surrounded by quintessence. *Eur. Phys. J. C* **2019**, *79*, 179. [CrossRef]

71.　Boonserm, P.; Visser, M. Bounding the greybody factors for Schwarzschild black holes. *Phys. Rev. D* **2008**, *78*, 101502. [CrossRef]

72.　Boonserm, P.; Ngampitipan, T.; Visser, M. Regge-Wheeler equation, linear stability, and greybody factors for dirty black holes. *Phys. Rev. D* **2013**, *88*, 041502. [CrossRef]

73.　Ngampitipan, T.; Boonserm, P. Bounding the Greybody Factors for Non-Rotating Black Holes. *Int. J. Mod. Phys. D* **2013**, *22*, 1350058. [CrossRef]

74.　Ngampitipan, T.; Boonserm, P. Bounding the greybody factors for the Reissner-Nordström black holes. *J. Phys. Conf. Ser.* **2013**, *435*, 012027. [CrossRef]

75.　Boonserm, P.; Chatrabhuti, A.; Ngampitipan, T.; Visser, M. Greybody factors for Myers-Perry black holes. *J. Math. Phys.* **2014**, *55*, 112502. [CrossRef]

76.　Nagar, A.; Rezzolla, L. TOPICAL REVIEW: Gauge-invariant non-spherical metric perturbations of Schwarzschild black-hole spacetimes. *Class. Quantum Gravity* **2005**, *22*, R167–R192. [CrossRef]